

The Turbulent Magnetic Prandtl Number of MHD Turbulence in Disks

Xiaoyue Guan and Charles F. Gammie¹

Astronomy Department, University of Illinois, 1002 West Green St., Urbana, IL 61801, USA

ABSTRACT

The magnetic Prandtl number Pr_M is the ratio of viscosity to resistivity. In astrophysical disks the diffusion of angular momentum (viscosity) and magnetic fields (resistivity) are controlled by turbulence. Phenomenological models of the evolution of large scale poloidal magnetic fields in disks suggest that the turbulent magnetic Prandtl number $\text{Pr}_{M,T}$ controls the rate of escape of vertical field from the disk; for $\text{Pr}_{M,T} \leq R/H$ vertical field diffuses outward before it can be advected inward by accretion. Here we measure field diffusion and angular momentum transport due to MHD turbulence in a shearing box, and thus $\text{Pr}_{M,T}$, by studying the evolution of a sinusoidal perturbation in the magnetic field that is injected into a turbulent background. We show that the perturbation is always stable, decays approximately exponentially, has decay rate $\propto k^2$, and that the implied $\text{Pr}_{M,T} \sim 1$.

Subject headings: accretion, accretion disks, magnetohydrodynamics

1. Introduction

Astrophysical disk evolution may be controlled in part by magnetic fields that are coherent over scales of order the radius R . Large scale fields are an essential element of theoretical models for the launching and collimation of disk winds (e.g. Blandford & Payne 1982; for a recent review see Pudritz et al. 2007), which lead to disk evolution because they exert direct torques on the surface of the disk. Large scale fields may also control the strength of turbulent angular momentum diffusion (in dimensionless form, α) within the disk, since numerical experiments in unstratified “shearing boxes” suggest that α is proportional to the

¹Physics Department, University of Illinois

mean field strength (e.g. Hawley et al. 1995). So what determines the strength of the large scale field in well ionized disks?

A few of the physical processes affecting the large scale field strength in thin disks can be easily listed: (1) advection of flux by large scale flows in the disk (e.g., inward advection by accretion, but also possibly meridional circulation); (2) turbulent diffusion; (3) dynamical interaction between large scale fields and large scale flows (e.g. enhanced accretion due to external torques); (4) control of small scale MHD turbulence by large scale fields (e.g. through the influence of a mean field on α); (5) generation of large scale fields by small scale MHD turbulence (a large scale dynamo); (6) introduction or removal of magnetic flux at the disk boundaries. These processes are difficult to study numerically because they involve nonsteady flows and a large dynamic range in length scale (R : scale height H) and time scale (viscous timescale : dynamical timescale).

A starting point for understanding large scale field evolution is the phenomenological model of Van Ballegoijen (1989; hereafter VB89). He considers a passive large scale field advected inward by accretion and diffused by turbulence in the disk (processes [1] and [2] above). Turbulence is modeled using a turbulent viscosity ν_T and turbulent resistivity η_T . The evolution of the poloidal field is then governed by the induction equation in vector potential form:

$$\partial_t A_\phi = \eta_T \partial_R \left[\frac{1}{R} \partial_R (R A_\phi) \right] + \eta_T \partial_z^2 A_\phi + v_R \frac{1}{R} \partial_R (R A_\phi), \quad (1)$$

where A_ϕ is the azimuthal component of the vector potential. A_ϕ labels field lines; when $\partial_t A_\phi \neq 0$ the field lines move radially through the disk with speed $\sim \partial_t A_\phi / \partial_R A_\phi$. In the limit that $\eta_T \rightarrow 0$ a vertical field would be advected inward by accretion and vertical field strength would increase with time. In the limit that $\nu \rightarrow 0$ the field lines simply diffuse out of the disk. Where do advection and diffusion balance?

VB89 give a surprising answer that can be understood as follows, assuming the field and disk are symmetric about the midplane. At the midplane the first term in (1) (radial diffusion of vertical field) is $\sim \eta_T B_z / R$, where $B_z = (1/R) \partial_R (R A_\phi)$ and we assume that $\partial_R \sim 1/R$. The second term (vertical diffusion of radial field, which can nevertheless cause radial motion of field lines) depends on the field geometry above and below the disk. If we assume the field lines enter and exit the disk at an angle of order unity (as in the wind model of Blandford & Payne 1982), $B_R = -\partial_z A_\phi \sim \mp B_z$ at $z = \pm H$ and $B_R = 0$ at the midplane, by symmetry. Then $\eta_T \partial_z^2 A_\phi \sim \eta_T B_z / H$. Using the usual viscous disk estimate $v_R \sim \nu / R$, the final term (field advection) is of order $\nu B_z / R$. To summarize, the terms on the right hand side of (1) are in the ratio $\eta_T B_z / R : \eta_T B_z / H : \nu B_z / R$. Evidently the first term is negligible in comparison to the second for a thin disk, provided the turbulent diffusion can

be described by a scalar diffusion coefficient. The second and third third can balance when $\nu_T/\eta_T \sim R/H$; diffusion and advection balance when $\text{Pr}_{M,T} \sim R/H$.

It is plausible that in disk turbulence $\text{Pr}_{M,T} \sim 1$ (e.g. Yousef et al. (2003)). Then outward field diffusion occurs on a timescale RH/ν . Large scale poloidal fields would vanish from the disk absent a dynamo that regenerates the field on the same timescale (process [5] above). Similar conclusions have been reached by Lubow et al. (1994) in the context of magnetically generated outflow/jet models. More complex models by Heyvaerts et al. (1996) also support such a picture.

There are of course ways to avoid the loss of large-scale field implied by the VB89 model, which is based on a purely phenomenological model for evolution of the disk and field. Spruit & Uzdensky (2005) discuss a model that reduces turbulent diffusion by grouping large scale vertical magnetic fields into bundles in the disk through flux expulsion. In these bundles the fields are strong enough to quench turbulence and thus avoid outward diffusion (processes [3] and [4] above). It has also been suggested by Uzdensky & Goodman (2008) that disk atmospheres might develop loop-like large scale coronal structures that delocalize disk evolution by transmitting angular momentum and energy. Rothstein & Lovelace (2008) consider the possibility that field diffusion is suppressed by a coronal layer where $v_A > c_s$, so that the MRI is suppressed and η_T is reduced. Another possibility is that disk evolution is driven by external torques associated with an MHD (Blandford-Payne type) wind running along the poloidal field lines. If the field is strong enough then the inflow speed v_R may be large enough to compete with outward diffusion of field lines even when $\text{Pr}_{M,T} \sim 1$ (process [3] above).¹ A final possibility is that $\text{Pr}_{M,T} \gg 1$.

In this paper we measure the turbulent magnetic Prandtl number $\text{Pr}_{M,T}$ directly from shearing box simulations. We infer the turbulent viscosity ν_T from the turbulent shear stress $w_{xy,T}$ (in dimensionless form, α), which controls diffusive radial transport of angular momentum in disks. We infer the turbulent resistivity η_T by tracking the evolution of a sinusoidal disturbance in the magnetic field that is imposed on an already turbulent state.

It is worth emphasizing that the turbulent Prandtl number $\text{Pr}_{M,T}$ is fundamentally different from the Prandtl number Pr_M associated with microscopic processes (e.g., Balbus & Henri

¹Although a naive estimate suggests this will not work. Suppose that the external torque per unit area $\tau \sim RM_{z\phi} \sim (\Sigma/H)R\langle v_A \rangle^2$, where $M_{ij} \equiv$ magnetic stress tensor, $\langle v_A \rangle \equiv$ the midplane Alfvén speed associated with the large scale field and $\Sigma \equiv$ surface density. Then the induced $v_r \sim \tau/(\Omega\Sigma R) \sim \langle v_A \rangle^2/c_s$, so in eq.(1) the second and third terms balance for $\eta_T \sim \langle v_A \rangle^2/\Omega$. If $\eta_T \sim \langle \delta v_A^2 \rangle/\Omega$ ($\delta v_A \equiv$ the Alfvén speed associated with disk turbulence), then (diffusion/advection) $\sim \langle \delta v_A^2 \rangle/\langle v_A \rangle^2$. Shearing box experiments suggest that this is large compared to 1 unless the poloidal field is so strong that turbulence is suppressed.

2008). Recent numerical experiments (Fromang & Papaloizou 2007; Lesur & Longaretti 2007) suggest that Pr_M can influence the saturation level of MRI driven disk turbulence at low Reynolds number.

The paper is organized as follows. In §2 we give a simple description of the local model and summarize our numerical algorithm. In §3 we describe the numerical procedure for measuring η_T . We report η_T and discuss its dependence on the model parameters. §4 We explain how we calculate $\text{Pr}_{M,T}$ and discuss our results.

2. Local Model and Numerical Methods

Our starting point is the local model for disks. It is obtained by expanding the equations of motion around a circular-orbiting coordinate origin at cylindrical coordinates $(r, \phi, z) = (r_o, \Omega_o t + \phi_o, 0)$, assuming that the peculiar velocities are comparable to the sound speed and that the sound speed is small compared to the orbital speed. The local Cartesian coordinates are obtained from cylindrical coordinates via $(x, y, z) = (r - r_o, r_o[\phi - \Omega_o t - \phi_o], z)$. We assume throughout that the disk is isothermal ($p = c_s^2 \rho$, where c_s is constant), and that the disk orbits in a Keplerian ($1/r$) potential.

In the local model the momentum equation of ideal MHD becomes

$$\frac{\partial \mathbf{v}}{\partial t} + \mathbf{v} \cdot \nabla \mathbf{v} + c_s^2 \frac{\nabla \rho}{\rho} + \frac{\nabla B^2}{8\pi\rho} - \frac{(\mathbf{B} \cdot \nabla)\mathbf{B}}{4\pi\rho} + 2\boldsymbol{\Omega} \times \mathbf{v} - 3\Omega^2 x \hat{\mathbf{x}} = 0. \quad (2)$$

The final two terms in equation (2) represent the Coriolis and tidal forces in the local frame. Our model is unstratified, which means that the vertical gravitational acceleration $-\Omega^2 z$ usually present in Keplerian disks is ignored. The box has size $L_x \times L_y \times L_z$.

Our model contains no explicit dissipation coefficients. Recent models with explicit scalar dissipation (Fromang & Papaloizou 2007, Lesur & Longaretti 2007) have shown that the saturated field strength in magnetized disk turbulence depends on the viscosity ν and resistivity η , and that **ZEUS** has an effective magnetic Prandtl number $\text{Pr}_{M,T} \equiv \nu/\eta \gtrsim 1$ (Fromang & Papaloizou 2007).

The orbital velocity in the local model is

$$\mathbf{v}_{orb} = -\frac{3}{2}\Omega x \hat{\mathbf{y}}. \quad (3)$$

This velocity, along with a constant density and zero magnetic field, is a steady-state solution to equation (2). If the computational domain extends to $|x| > (2/3)H = (2/3)c_s/\Omega$, then the orbital speed is supersonic with respect to the grid.

The local model can be studied numerically using the “shearing box” boundary conditions (e.g. Hawley et al. 1995). The boundary conditions on the y boundaries of the box are periodic, while the x boundaries are “nearly periodic”, i.e. they connect the radial boundaries in a time-dependent way that enforces the mean shear flow. We also use periodic boundary conditions in the vertical direction; this is the simplest possible version of the shearing box model.

Our models are evolved using **ZEUS** (Stone & Norman 1992). **ZEUS** is an operator-split, finite difference scheme on a staggered mesh. It uses artificial viscosity to capture shocks.² For the magnetic field evolution **ZEUS** uses the Method of Characteristics-Constrained Transport (MOC-CT) scheme, which is designed to accurately evolve Alfvén waves (MOC) and to preserve the $\nabla \cdot \mathbf{B} = 0$ constraint to machine precision (CT).

We have modified **ZEUS** to include “orbital advection” (Masset 2000; Gammie 2001; Johnson & Gammie 2005) with a magnetic field (Johnson et al. 2008). Advection by the orbital component of the velocity \mathbf{v}_{orb} (which may be supersonic with respect to the grid) is done using interpolation. With this modification the timestep condition $\Delta t < C\Delta x/(|\delta\mathbf{v}| + c_{max})$ ($c_{max} \equiv$ maximum wave speed and $C \equiv$ Courant number) depends only on the perturbed velocity $\delta\mathbf{v} = \mathbf{v} - \mathbf{v}_{orb}$ rather than \mathbf{v} . So when $|\mathbf{v}_{orb}| \gtrsim c_{max}$ (for shearing box models with $v_A^2/c_s^2 \lesssim 1$, when $L \gtrsim H$) the timestep can be larger with orbital advection, and computational efficiency is improved.

Orbital advection also improves accuracy. **ZEUS**, like most Eulerian schemes, has a truncation error that increases as the speed of the fluid increases in the grid frame. In the shearing box without orbital advection the truncation error would then increase monotonically with $|x|$. Orbital advection reduces the amplitude of the truncation error and also makes it more nearly uniform in $|x|$ (Johnson et al. 2008).

We have also implemented an additional procedure to remove the radially dependent numerical dissipation in large shearing box simulations that was reported in Johnson et al. (2008). We do so by systematically shifting the entire box by a few grid points in the radial direction at $t = n2L_y/(3\Omega L_x)$, $n = 1, 2, 3, \dots$ (this is when the shearing box boundary conditions are exactly periodic). After the shift we execute a divergence cleaning procedure to remove the monopoles that build up due to truncation error along the radial boundaries of the shearing box in our implementation of the shearing box boundary conditions, which remaps the EMFs rather than the magnetic field. We do this by gathering $s = \nabla \cdot \mathbf{B}$

²A Von-Neumann Richtmyer artificial viscosity is a pressure proportional to $(\nabla \cdot \mathbf{v})^2$ that is small outside shocks. It should not be confused with the “anomalous viscosity” used to model turbulent angular momentum diffusion in standard accretion disk theories (Shakura & Sunyaev 1973; Lynden-Bell & Pringle 1974).

onto a single processor, solving the Poisson equation $\nabla^2\psi = s$ using a standard FFT-based procedure, and then setting $\mathbf{B} \rightarrow \mathbf{B} - \nabla\psi$. The additional computational cost is negligible (usually less than 0.1% of the total cost) because the operation is performed infrequently. Johansen et al. (2008) have discussed other techniques to eliminate the radial dependence of numerical diffusion. This procedure eliminates the features reported in Johnson et al. (2008).

3. Turbulent Resistivity

Our focus is on the diffusive effects of MHD turbulence induced by the magnetorotational instability (MRI; Balbus & Hawley 1991). All models in this section have a mean toroidal field $\langle \mathbf{B} \rangle = B_0 \hat{\mathbf{y}}$, where B_0 is chosen so that the initial plasma parameter $\beta \equiv 8\pi P_0/B_0^2 = 400$. The models are evolved long enough (≥ 40 orbits) to reach a saturated (statistically steady) state.

First we consider radial diffusion of a vertical field. Although this is the subdominant term in eq.(1), it is easier to measure (for reasons we will discuss shortly) and thus allows us to explore systematic effects related to resolution, scale of the perturbation, and details of the initial state more readily.

To measure the turbulent resistivity we evolve an initial state containing a mean field for hundreds of orbits. We then (arbitrarily) select an instant to inject a magnetic field perturbation of the form

$$\delta \mathbf{B}_z = a \sin(k_x x) \hat{\mathbf{z}}. \quad (4)$$

Here $k_x = 2\pi n_x/L_x$ is the radial wavenumber for the perturbation. We consider models with $4 < L_x/H < 32$. We choose a so that it is larger than the background turbulent fluctuations³, but small enough so that it does not greatly affect the background turbulence. Here we use $0.1 < a/B_0 < 0.8$. We then evolve the perturbed turbulence self-consistently, taking the sine transform of \mathbf{B}_z to obtain $a(t)$.

A typical evolution $a(t)$ is shown in Figure 1. The initial decay is approximately exponential. We measure a decay rate $1/\tau$ by fitting an exponential to $a(t)$ over at least one e-folding time. The decay rates are listed in Table 1. To give a sense of the amplitude of fluctuations in the background state we also plot in Figure 1 the evolution of the cosine

³The background contains power in the magnetic field at small wavenumber, with the power spectrum $\delta B_k^2 \sim \text{const.} \sim \langle \delta B^2 \rangle \lambda^3$, where λ is a correlation length (see Guan et al. 2008 for a discussion). This implies that the Fourier series coefficients in the background state will have rms amplitude $\langle \delta B^2 \rangle^{1/2} (\lambda^3 / (L_x L_y L_z))^{1/2}$

amplitude; since the cosine amplitude remains so much smaller than the sine amplitude it is clear that the decay of $a(t)$ is not simply due to phase drift. Eventually $a(t)$ decays to the background level. In every case we have examined the perturbation decayed; the turbulence was stable to a large-scale magnetic field perturbation.

Before going on we need to determine how strongly our measurement of τ depends on our selection of initial conditions. We therefore measure τ for an ensemble of initial conditions selected from the same run at widely separated times. We have done this for three models (s2, s5, and n1). The variation in τ is $\leq 13\%$, which may then be regarded as an error bar on our measurement.

The decay time τ is related to η_T as follows. Solving the induction equation with a scalar resistivity,

$$a = a_0 \exp(-\eta_T k_x^2 t), \quad (5)$$

so we define

$$\eta_T \equiv (k_x^2 \tau)^{-1}. \quad (6)$$

Values of η_T are given in Table 1. In general η_T will depend on the magnitude and direction of \mathbf{k} and on the background field $\langle \mathbf{B} \rangle$.

Does the decay time scale as k_x^{-2} , i.e. does η_T depend on the magnitude of \mathbf{k} ? In a model with $(L_x, L_y, L_z) = (8, 4\pi, 2)H$ we imposed perturbations with $n_x = 1, 2, 3$ on the same initial state. We find $\tau = 32.7, 10.4, 4.93$ respectively, so that $\eta_T = 0.0495, 0.0388, 0.0366$, crudely consistent with a diffusive scaling. Models n1, s5, and s6, with $n_x = 1$ but $L_x = 8, 16, 32$ and identical numerical resolution, have $\eta_T = 0.0495, 0.0330, 0.0304$, again crudely consistent with a diffusive scaling. So it appears that η_T is at most very weakly dependent on the magnitude of \mathbf{k} .

We checked the effect of resolution in models with N_x/L_x ranging from $32/H$ to $128/H$. In all the runs $\Delta x = \Delta z \simeq 2\Delta y$ (except in model s4, where $\Delta x = \Delta z = \Delta y$; varying the zone aspect ratio made no difference in η_T) and $(L_x, L_y, L_z) = (4, 2\pi, 1)H$. Comparing runs r1, r2, and r3, we find $\eta_T = 0.037, 0.035$ and 0.034 respectively. Our measurement of η_T is thus consistent with convergence, since the variation with resolution is smaller than the noise in decay time measurement that arise from choosing a particular initial state.

We found that η_T *does* depend on the field perturbation strength a_0 . In the $(L_x, L_y, L_z) = (8, 4\pi, 2)H$ models with the same wavelength perturbation and a fixed resolution, when a_0 increases from $0.1B_0$ to $0.4B_0$, η_T increases slightly ($\sim 20\%$) with a_0 ; when $a_0 = 0.8B_0$ η_T almost doubles. This is not surprising. It is known that the velocity fluctuation amplitude in shearing boxes increases in the presence of a background mean field. For sufficiently long wavelength sinusoidal perturbations, the imposed vertical fields looks, locally, like a mean

field and so increases the velocity fluctuation amplitude and therefore η_T .

We did not find any dependence of η_T on box size. Comparing runs with $L_x/H = 4$ and $L_y/H = 2\pi, 4\pi, 8\pi$ we found $\eta_T \simeq 0.03$ in every case. Comparing runs with $L_x/H = 4$ to 32, we again see that η_T lies in a narrow range around 0.03. Notice that for a vertical field perturbation with $\lambda_x < 4H$ the decay time is less than Ω^{-1} .

But what of the dominant term in eq(1), the vertical diffusion of radial field? It is unclear how to measure this in the shearing box because the radial field is always buried “in the disk”, where it is continually sheared into azimuthal field by the background shear (in a stratified disk the radial field is present above and below the disk, where the Alfvén speed is high and the plasma will corotate along field lines). So instead we measured the vertical diffusion of azimuthal field. This is also relevant to wind models because the radial field above and below the disk is always accompanied by an azimuthal field.

To measure the azimuthal field diffusion we inject a perturbation of the form

$$\delta \mathbf{B}_y = a \sin(k_z z) \hat{\mathbf{y}} \quad (7)$$

into an already turbulent state, measure the decay time τ , and set

$$\eta_T = (k_z^2 \tau)^{-1}. \quad (8)$$

We imagine a large scale field entering the disk at a inclination of ~ 30 deg, running vertically through the midplane, and leaving at a similar inclination; to mimic this geometry we set $2\pi/k_z = L_z = 4H$ and $2H$.

The perturbation amplitude must be chosen larger than the turbulent background but as small as possible so it does not influence the background state. Because the turbulent fluctuations in the azimuthal field are larger than the fluctuations in the vertical field, a in eq.(7) must be an order of magnitude larger (in comparison to B_0) than a in eq.(4).

Model v1 and v2 (see Table 1) have $(L_x, L_y, L_z) = (4, 4\pi, 4)H$ and resolution $128 \times 200 \times 128$; v1 has $a_0 = 2B_0$ while v2 has $a_0 4B_0$. We found $1/\tau = 0.052$ and 0.050 respectively. This corresponds to a vertical diffusion coefficient $\eta_T \sim 0.020$. Details are given in Table 1.

To test for resolution dependence we repeated the above experiment at resolution $256 \times 400 \times 256$, with $a_0 = 4B_0$ (model v3 in Table 1). We found $1/\tau = 0.040$ and thus $\eta_T \sim 0.016$. This diffusion coefficient is $\sim 20\%$ smaller than that obtained at lower resolution. This small decrease in η_T is mainly caused by slightly lower turbulent saturation level in the high resolution run in the perturbed state, where the saturation α is about 25% smaller. This might be surprising because on average higher resolution runs have higher saturation levels (see, e.g., Guan et al. 2009), but α fluctuates in time; our α is averaged over the same time interval used to fit $1/\tau$.

4. Discussion: Turbulent Magnetic Prandtl number

To calculate $\text{Pr}_{\text{M,T}}$, we need to assign a “viscosity” to the turbulence. We do this by measuring the turbulent shear stress

$$w_{xy,T} = \langle \rho v_x \delta v_y - \frac{B_x B_y}{4\pi} \rangle \quad (9)$$

and equating this to the shear stress that would be measured in a viscous fluid

$$w_{xy,v} = \rho \nu q \Omega, \quad (10)$$

where $q \equiv -(1/2)d \ln \Omega^2 / d \ln R = 3/2$ for a Keplerian potential. Thus

$$\nu = \frac{w_{xy,T}}{\rho q \Omega}. \quad (11)$$

and the turbulent magnetic Prandtl number

$$\text{Pr}_{\text{M,T}} \equiv \frac{\nu_{\text{T}}}{\eta_{\text{T}}} = (\tau \Omega) (kH)^2 \frac{w_{xy,T}}{q \langle \rho \rangle c_s^2}. \quad (12)$$

The turbulent shear stress $w_{xy,T}$ is related to α by $\alpha \equiv w_{xy,T} / \langle \rho \rangle c_s^2$. The evolution of α from one of our runs is shown in Figure 1.

We measure the time average of α during the decay time, denoted $\bar{\alpha}$ (over the same period we fit τ), and use equation (12) to calculate $\text{Pr}_{\text{M,T}}$. The results are compiled in Table 1. The vertical field experiments give $0.35 < \text{Pr}_{\text{M,T}} < 0.58$. The azimuthal field experiments give $\text{Pr}_{\text{M,T}} \sim 1$.

In the current limited set of simulations we see no clear sign of $\text{Pr}_{\text{M,T}}$ scaling with model or numerical parameters. This consistency is remarkable when we look at the radial diffusion of vertical field with different perturbation field strength a_0 . In the $(L_x, L_y, L_z) = (8, 4\pi, 2)H$ models when the perturbation amplitude is strong, as in the $a_0 = 0.8B_0$ case, both η and $w_{xy,T}$ double compared to their weakly perturbed counterparts with $a_0 = 0.1B_0$; this doubling is precisely what is required for a constant $\text{Pr}_{\text{M,T}}$.

We have also carried out comparison experiment with slightly larger initial toroidal field strength B_0 ($\beta_0 = 100$; model b2a in Table 1). Past numerical experiments (Hawley et al. 1995; Guan et al. 2008) imply that the saturation level scales linearly with B_0 . For this model we found $\bar{\alpha} = 0.0568$ and $\eta_{\text{T}} = 0.0878$. Both the turbulent saturation level and η_{T} double, giving $\text{Pr}_{\text{M,T}} \sim 0.43$.

Recently Lesur & Longaretti (2008) have measured the turbulent resistivity in shearing box simulations. Their technique for measuring turbulent resistivity differs from ours: they

directly measure the EMF required to maintain a particular sinusoidal variation in the field, they measure a resistive stress tensor, and they consider only a mean vertical field (rather than the mean azimuthal field considered here). They find $\text{Pr}_{\text{M,T}} = 1.6$ for the diffusion of a radially varying azimuthal field.

Transport properties of the MRI-generated turbulent flow have also been studied in the context of dust (passive scalar) mixing in a shearing box (Carballido et al. 2005; Johansen & Klahr 2005; Johansen et al. 2006; Turner et al. 2006; Fromang & Papaloizou 2006). The analog of $\text{Pr}_{\text{M,T}}$ in these experiments is the turbulent Schmidt number $\text{Sc} \equiv \nu_{\text{T}}/D_{\text{T}}$, where D_{T} is the diffusion coefficient for the grains. In models with zero net magnetic flux (either when the dust is modeled as a passive scalar (Turner et al. 2006), or when the dust is coupled to the gas by drag (Johansen & Klahr 2005; Fromang & Papaloizou 2006)), $\text{Sc} \sim 1$. In models with a net vertical flux (Carballido et al. 2005; Johansen et al. 2006), Sc was found to be anisotropic and increase with α (and therefore depend on the initial vertical field strength), ranging from $\text{Sc} \sim 1$ for a weak field, to $\text{Sc} \sim 2$ for radial diffusion $\text{Sc} \sim 10$ for vertical diffusion when the mean field is strong and $\alpha \sim 0.5$. Our results are broadly consistent with these measurements in the sense that $\text{Sc} \sim \text{Pr}_{\text{M,T}}$ when the mean field is weak. Our scheme for measuring $\text{Pr}_{\text{M,T}}$ is much more computationally expensive when the turbulence is strong, because a large computational volume is required to reduce the background fluctuations. It would be interesting to investigate whether $\text{Pr}_{\text{M,T}} \sim 10$ can be achieved with strong background fields in future investigations.

A $\text{Pr}_{\text{M,T}}$ of order of unity is not surprising, perhaps, from a turbulent mixing point of view. Parker (1979), for example, argued that in isotropic turbulence $\nu_{\text{T}} \sim \eta_{\text{T}} \sim lv$, where l is the largest dimension of eddies in the MHD turbulent flow and v is the characteristic eddy turnover speed. Interestingly, Yousef et al. (2003) also obtained an order of unity $\text{Pr}_{\text{M,T}}$ from their turbulence simulations, where the turbulence is sustained by external forcing rather than the MRI in a disk.

Can large scale magnetic fields avoid escape from turbulent disks? We clearly have not included all of the effects outlined in the introduction that might influence the evolution of large scale fields. Of these, perhaps the simplest route to large scale fields is a rapid accretion mode in which the mean field torques the disk, causing it to accrete more rapidly than would a viscous disk. But our results cast doubt on models that confine the large scale field by setting $\text{Pr}_{\text{M,T}} \sim R/H$ (e.g. Shu et al. (2007)).

Our models do not show a clear scaling of $\text{Pr}_{\text{M,T}}$ with model parameters, but the dynamic range in parameters (and thus in η_{T}) is small; future experiments over a broader range of initial field strengths may show scaling that is not evident here. Our models also do not include an explicit dissipation model, on which $\text{Pr}_{\text{M,T}}$ might also depend.

This work was supported by the National Science Foundation under grants AST 00-93091, PHY 02-05155, and AST 07-09246, and a Sony Faculty Fellowship, a University Scholar appointment, and a Richard and Margaret Romano Professorial Scholarship to CFG. We are grateful to Shane Davis, Stu Shapiro and Fred Lamb for discussions. We also thank Ethan Vishniac and an anonymous referee for helpful suggestions. High resolution simulations were performed on the Turing cluster at the CSE program in UIUC and Lonestar cluster at TACC.

REFERENCES

- Balbus, S. A., & Hawley, J. F. 1991, *ApJ*, 376, 214
- Balbus, S. A., & Henri, P. 2008, *ApJ*, 674, 408
- Blandford, R. D. & Payne, D. G. 1982 *MNRAS*, 199, 883
- Carballido, A., Stone, J. M., & Pringle, J.E. 2005, *MNRAS*, 358, 1055
- Colella, P. 1990, *Journal of Computational Physics*, 87, 171
- Fromang, S., & Papaloizou, J. 2007 *A&A*, 452, 751
- Fromang, S., & Papaloizou, J. 2007 *A&A*, 476, 1113 (FP07)
- Guan, X., Gammie, C. F., Simon, J. B., & Johnson, B. M. 2008 *ApJ* submitted
- Gammie, C. F. 2001, *ApJ*, 553, 174
- Hawley, J. F., Gammie, C. F., & Balbus, S. A. 1995, *ApJ*, 440, 742
- Heyvaerts, J., Priest, E. R. & Bardou, A. 1996, *ApJ*, 473, 403
- Johansen, A., & Klahr, H. 2005, *ApJ*634, 1353
- Johansen, A., Klahr, H., & Mee, A. J. 2006, *MNRAS*, 370, L71
- Johansen, A., Klahr, H., & Youdin, A. 2008, [astro-ph/0811.3937](https://arxiv.org/abs/0811.3937)
- Johnson, B. M., & Gammie, C. F. 2005, *ApJ*, 635, 149
- Johnson, B. M., Xiaoyue Guan, & Gammie, C. F. 2008, *ApJS*, 177, 373
- Lesur, G. & Longareti, P. Y. 2007, *A&A*, 378, 1471
- Lesur, G. & Longareti, P. Y. 2008, in *Proceedings of the Annual meeting of the French Society of Astronomy and Astrophysics*, ed. C. Charbonnel, F. Combes, & R. Sama, 491
- Lynden-Bell, D., & Pringle, J. E. 1974, *MNRAS*, 235, 269
- Lubow, S. H., Papaloizou, J. C. B., & Pringle, J. E. 1994, *MNRAS*, 267, 235
- Masset, F. 2000, *A&AS*, 141, 165
- Parker, E. N. 1979, Chapter 17, *Cosmical Magnetic Fields*. Clarendon Press, Oxford

- Pudritz, R. E., Ouyed, R., Fendt, Ch., & Brandenburg, A. 2007, in *Protostars and Planets V*, ed. B. Reipurth, D. Jewitt, & K. Keil (Tucson: University of Arizona Press), 277
- Rothstein, D. M. & Lovelace, R. V. E. 2008, *ApJ*, 677, 1221
- Shakura, N. I., & Sunyaev, R. A. 1973, *A&A*, 24, 337
- Shu, F. H., Galli, D., Lizano, S., Glassgold, A. E., & Diamond, P. H. 2007, *ApJ*, 665, 535
- Stone, J. M. & Norman, M. L. 1992, *ApJS*, 80, 753
- Spruit, H. C., & Uzdensky, D. A. 2005, *ApJ*, 629, 960
- Turner, N. J., Willacy, K., Bryden, G., & Yorke, H. W. 2006, *ApJ*, 639, 1218
- Uzdensky, D. A., & Goodman, J. 2008, *ApJ*, 682, 608
- van Ballegoijen, A. A. 1989, *Accretion Disks and Magnetic Fields in Astrophysics*, 156, 99
- Yousef, T. A., Brandenburg, A., & Rüdiger, G. 2003, *A&A*, 411, 321
- Yousef, T. A., Heinemann, T., Schekochihin, A. A., Kleeorin, N., Rogachevskii, I., Iskakov, A. B., Cowley, S. C., & McWilliams, J. C. 2008, *Phys. Rev. Lett.*, 100, 184501

Table 1. Model Parameters

Model	Size	Resolution	β_0	a_0/B_0	n_x	$\bar{\alpha}$	$1/\tau$	η_T	$\text{Pr}_{M,T}$
Radial Diffusion of a Vertical Field									
size									
s1	$(4, 2\pi, 1)H$	$64/H$	400	0.2	1	0.0232	0.0758	0.0307	0.50
s2	$(4, 4\pi, 1)H$	$64/H$	400	0.2	1	0.0235	0.0660	0.0268	0.58
s3	$(4, 8\pi, 1)H$	$64/H$	400	0.2	1	0.0238	0.0740	0.0300	0.53
s4	$(8, 2\pi, 1)H$	$64/H$	400	0.2	1	0.0198	0.0194	0.0314	0.42
s5	$(16, 2\pi, 1)H$	$32/H$	400	0.2	1	0.0209	0.00509	0.0330	0.42
s6	$(32, 2\pi, 1)H$	$32/H$	400	0.2	1	0.0210	0.00117	0.0304	0.46
<hr/>									
n_x									
n1	$(8, 4\pi, 2)H$	$32/H$	400	0.2	1	0.0262	0.0306	0.0495	0.35
n2	$(8, 4\pi, 2)H$	$32/H$	400	0.2	2	0.0252	0.0957	0.0388	0.43
n3	$(8, 4\pi, 2)H$	$32/H$	400	0.2	3	0.0240	0.203	0.0366	0.44
<hr/>									
a_0									
a1	$(8, 4\pi, 2)H$	$32/H$	400	0.1	1	0.0239	0.0268	0.0434	0.37
a2	$(8, 4\pi, 2)H$	$32/H$	400	0.2	1	0.0262	0.0306	0.0495	0.35
a3	$(8, 4\pi, 2)H$	$32/H$	400	0.4	1	0.0338	0.0315	0.0511	0.44
a4	$(8, 4\pi, 2)H$	$32/H$	400	0.8	1	0.0604	0.0496	0.0804	0.50
<hr/>									
resolution									
r1	$(4, 2\pi, 1)H$	$32/H$	400	0.4	1	0.0226	0.0921	0.0373	0.40
r2	$(4, 2\pi, 1)H$	$64/H$	400	0.4	1	0.0274	0.0875	0.0355	0.51
r3	$(4, 2\pi, 1)H$	$128/H$	400	0.4	1	0.0239	0.0840	0.0340	0.47
<hr/>									
β_0									
b1	$(8, 4\pi, 2)H$	$32/H$	400	0.2	1	0.0262	0.0306	0.0495	0.35
b2a	$(8, 4\pi, 2)H$	$32/H$	100	0.2	1	0.0568	0.0541	0.0878	0.43
b2b	$(8, 4\pi, 2)H$	$32/H$	100	0.4	1	0.0607	0.0463	0.0750	0.54
<hr/>									
Vertical Diffusion of an Azimuthal Field									
v1	$(4, 4\pi, 4)H$	$32/H$	400	2.0	1	0.0313	0.0521	0.0211	0.99
v2	$(4, 4\pi, 4)H$	$32/H$	400	4.0	1	0.0386	0.0503	0.0204	1.26
v3	$(4, 4\pi, 4)H$	$64/H$	400	4.0	1	0.0288	0.0400	0.0162	1.18
v4	$(8, 4\pi, 2)H$	$32/H$	400	4.0	1	0.0276	0.1425	0.014	1.27

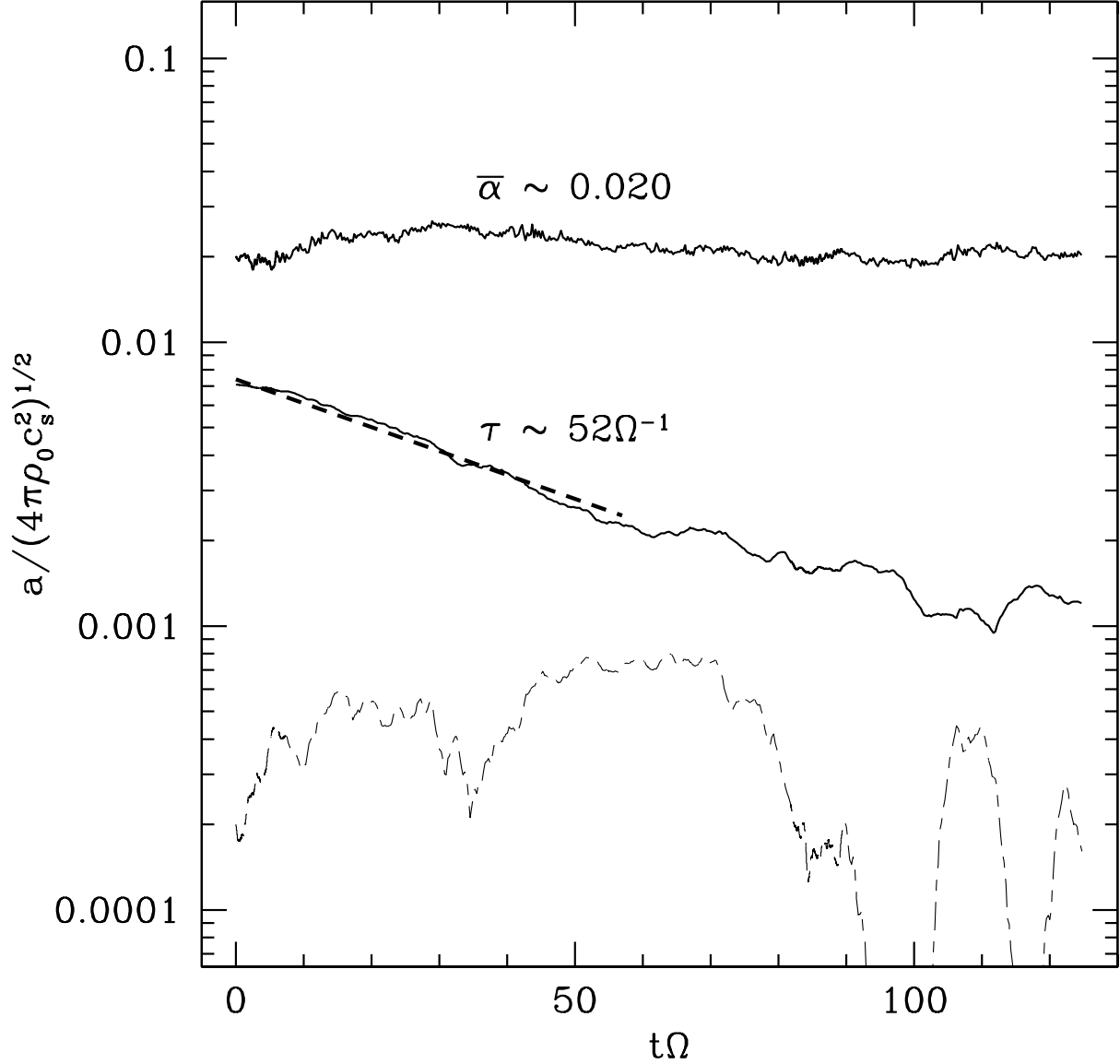


Fig. 1.— Evolution of the amplitude a of a magnetic field perturbation $\delta B_z = a \sin(k_x x)$ in the presence of MHD turbulence (lower solid line; model s4). A linear fit to $\ln a(t)$ is shown as a heavy dashed line. The decay time is $\tau \sim 52\Omega^{-1}$, implying a turbulent resistivity $\eta_T \sim 0.031$. Also shown is the evolution of α in the same experiment (upper solid line). The turbulent magnetic Prandtl number $\text{Pr}_{M,T} \sim 0.42$. The dashed line shows the evolution of the corresponding cosine amplitude in δB_z , indicating the amplitude of large scale field fluctuations in the turbulent background.